

Contribution from the Department of Chemistry,
Harvard University, Cambridge, Massachusetts 02138

Subsite-Differentiated Analogues of Biological [4Fe-4S] Clusters Effected by Binding of a Macrocyclic Polyether Trithiol

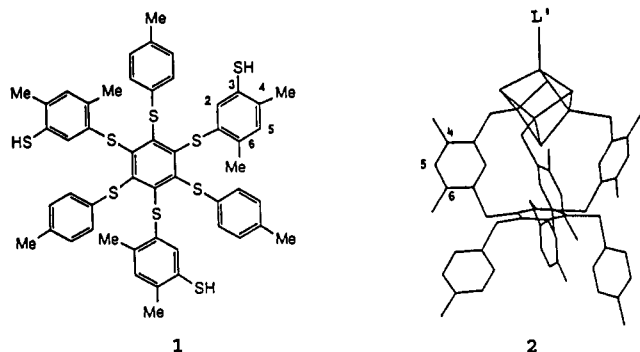
M. A. Whitener, Gang Peng, and R. H. Holm*

Received December 13, 1990

The macrocyclic polyether trithiol **7** (c-L(SH)₃) was synthesized in five steps from resorcinol. The cyclic structures of the tris (1,3-phenylene) crown ether (**5**) and protected trithiol (**6**) intermediates were demonstrated by X-ray methods. Compound **5** (C₂₆H₂₈O₆) crystallizes in the monoclinic space group *P*2₁/*c*, with *a* = 10.318 (5) Å, *b* = 17.333 (5) Å, *c* = 13.653 (5) Å, β = 111.31 (3)°, and *Z* = 4. Compound **6**-Et₂O (C₅₁H₅₆O₇S₃) crystallizes in the monoclinic space group *P*2₁/*n*, with *a* = 14.315 (9) Å, *b* = 12.823 (8) Å, *c* = 25.56 (1) Å, β = 90.94 (5)°, and *Z* = 4. Reaction of **7** with [Fe₄S₄(SEt)₄]²⁻ in acetonitrile results in quantitative cluster capture and the formation of [Fe₄S₄(c-LS₃)(SEt)]²⁻ (**8**), in which the Fe subsites are differentiated in a 3:1 ratio. Treatment of **8** with pivaloyl chloride affords [Fe₄S₄(c-LS₃)Cl]²⁻ (**9**). This cluster reacts with a variety of ligands to generate the site-differentiated clusters [Fe₄S₄(c-LS₃)L']²⁻, with L' = *p*-MeC₆H₄S⁻, CN⁻, tacn, (*t*-BuNC)₃, and a probable sulfide-bridged double cubane cluster (L' = 1/2S²⁻). Reactions were monitored by ¹H NMR spectroscopy, which detected cluster substitution because of the sensitivity of isotropic shifts to variations in the ligands L' at the unique site. In all cases, the spectra were consistent with mirror symmetry, indicating trithiolate ligand binding to a single [Fe₄S₄]²⁺ core unit. Isotropic shifts and [Fe₄S₄]^{2+/+} redox potentials are tabulated. Deprotonated trithiol **7** is the second trithiolate ligand shown to form subsite-differentiated cubane-type clusters and to support subsite-specific substitution reactions. Properties of the clusters [Fe₄S₄(c-LS₃)L']²⁻ and the previously reported [Fe₄S₄(LS₃)L']²⁻ species, derived from a trithiol of different structure and conformational rigidity, are similar at constant L'. This suggests that neither tridentate ligand imposes a highly specific environment on the Fe₄S₄ core and thus indicates that either ligand may be utilized in the chemistry of subsite-differentiated clusters with comparable results.

Introduction

The deprotonated trithiol L(SH)₃ (**1**) functions as a semirigid tridentate cavating ligand toward Fe₄S₄ and other cubane-type clusters.¹⁻³ When bound, it effects a 3:1 iron subsite differen-



tiation, which has been proven in the solid state by X-ray analysis^{1,2} and in solution by ¹H NMR spectroscopy.¹⁻³ With the Fe₄S₄ clusters **2**, this has permitted investigations of the intrinsic ligand binding properties and structural and electronic features specific to the unique subsite. These studies have included demonstration of binding of a wide variety of mono-, bi-, and tridentate ligands,¹⁻⁷ the formation of and interactions between bridged clusters,⁵ modulation of redox potentials and charge distribution by substitution of ligand L',⁶ and stabilization of the *S* = 2 [Fe₃S₄]⁰ cluster fragment by binding of strong field ligands.⁷ Certain of these clusters provide synthetic analogues for native clusters that manifest subsite-specific properties. Such properties have been analyzed elsewhere.⁸

While the clusters **2** have been uniquely valuable in the elucidation of iron subsite-specific properties, we wished to obtain an alternative synthetic representation of subsite-differentiated clusters in order to address several points that remain at issue. One of these is the intrinsic effect of the unusual ligand structure on cluster properties. In **2**, the three coordinating "arms" are buttressed in positions on the same side of the central benzene ring by the *p*-tolylthio "legs", which are disposed on the other side. The Fe₄S₄ core is positioned partly within a hydrophobic cavity whose walls are the near edges of the phenyl rings in the arms and whose floor is the central ring. A detailed conformational analysis of cluster structure is presented elsewhere.² A second point is that we have been unable to stabilize the cuboidal Fe₃S₄ core, proven to exist in protein-bound form,⁹⁻¹¹ by use of ligand **1**. While not all experiments are complete, the status thus far makes desirable another type of trithiolate ligand having a different conformation and dimensions and dissimilar stereochemical rigidity. Here we report the synthesis of such a ligand and its Fe₄S₄ cluster capture reaction and demonstrate that it supports reactions specific to the unique subsite.

Experimental Section

Preparation of Compounds. All manipulations and operations were conducted under a pure dinitrogen atmosphere. Solvents were dried and degassed by standard procedures. 1,2-Dibromoethane and 1,3-dibromopropane were distilled before use and stored over 4-Å molecular sieves. Melting points are uncorrected. Compound numbers refer to Figures 1 and 2.

Cyclic Trithiol Ligand. (a) 3,3-[1,2-Ethanedilybis(oxy)]bis(phenol) (**3**). A mixture of 240 g (2.18 mol) of resorcinol and 72 g (0.38 mol) of 1,2-dibromoethane in 60 mL of water was brought to reflux. Over a period of 3 days, 50 g (0.76 mol) of KOH in 100 mL of water was added to the refluxing solution. After the addition was complete, the solution was stirred for 2 h and poured into 6 L of water to which had been added 100 mL of concentrated H₂SO₄. The solution was stirred vigorously for 2 h, and the solid that separated was collected by filtration and washed with water. Recrystallization from hot water afforded the pure product as 25 g (30%) of white needles, mp 161–163 °C (lit.¹² mp 163 °C). ¹H

- (1) Stack, T. D. P.; Holm, R. H. *J. Am. Chem. Soc.* **1987**, *109*, 2546; **1988**, *110*, 2484.
- (2) Stack, T. D. P.; Weigel, J. A.; Holm, R. H. *Inorg. Chem.* **1990**, *29*, 3745.
- (3) Ciurli, S.; Holm, R. H. *Inorg. Chem.* **1989**, *28*, 1685.
- (4) Weigel, J. A.; Holm, R. H. *J. Am. Chem. Soc.*, in press.
- (5) Stack, T. D. P.; Carney, M. J.; Holm, R. H. *J. Am. Chem. Soc.* **1989**, *111*, 1670.
- (6) Ciurli, S.; Carriè, M.; Weigel, J. A.; Carney, M. J.; Stack, T. D. P.; Papaefthymiou, G. C.; Holm, R. H. *J. Chem. Soc.* **1990**, *112*, 2654.
- (7) (a) Weigel, J. A.; Holm, R. H.; Surerus, K. K.; Münck, E. *J. Am. Chem. Soc.* **1989**, *111*, 9246. (b) Weigel, J. A.; Holm, R. H.; Srivastava, K. K. P.; Münck, E. *J. Am. Chem. Soc.* **1990**, *112*, 8015.

- (8) Holm, R. H.; Ciurli, S.; Weigel, J. A. *Prog. Inorg. Chem.* **1990**, *38*, 1.
- (9) Kissinger, C. R.; Adman, E. T.; Sieker, L. C.; Jensen, L. H. *J. Am. Chem. Soc.* **1988**, *110*, 8721.
- (10) Stout, C. D. *J. Biol. Chem.* **1988**, *263*, 9256; *J. Mol. Biol.* **1989**, *205*, 545.
- (11) Robbins, A. H.; Stout, C. D. *Proc. Natl. Acad. Sci. U.S.A.* **1989**, *86*, 3639; *Proteins* **1989**, *5*, 289.
- (12) Kohn, M.; Wilhelm, F. *Monatsh. Chem.* **1922**, *43*, 545.

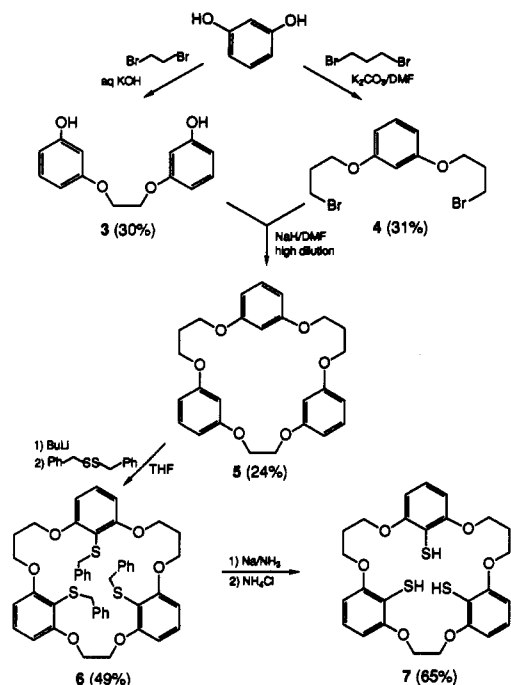


Figure 1. Synthetic scheme for the macrocyclic polyether trithiol 7.

NMR (acetone- d_6): δ 4.24 (s, 4), 6.39–6.42 (m, 6), 7.05 (t, 1), 8.27 (s, 2, OH).

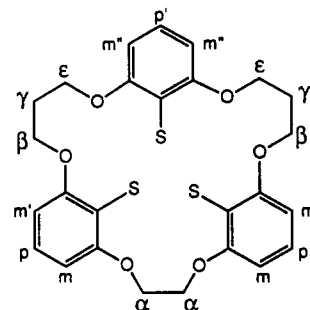
(b) **1,3-Bis[(3-Bromopropyl)oxy]benzene (4)**. To a degassed solution of 27.5 g (0.25 mol) of resorcinol and 202 g (1.00 mol) of 1,3-dibromopropane in 500 mL of DMF was added 138 g (1.00 mol) of K_2CO_3 . The mixture was stirred at ambient temperature overnight and filtered. The filtrate was mixed with 400 mL of dichloromethane, and the solution was washed with saturated aqueous NaCl solution. The organic layer was washed with 10% aqueous NaCl solution and then with a saturated NaCl solution and dried ($MgSO_4$). Solvent was removed in vacuo to leave a reddish waxy solid. This material was distilled at 167 °C (10 mmHg), and the solidified distillate was recrystallized from hot ethanol, resulting in 27 g (31%) of pure product as white flakes, mp 65–67 °C (lit.¹³ mp 67 °C). 1H NMR ($CDCl_3$): δ 2.31 (t, 4), 3.60 (t, 4), 4.09 (t, 4), 6.49 (d/d, 2), 6.53 (d, 1), 7.18 (t, 1). This compound has been previously prepared on a much larger scale in 25% yield.¹³

(c) **Macrocyclic Polyether (5)**. A solution of 7.0 g (28.4 mmol) of 2 and 10.0 g (28.4 mmol) of 3 in 50 mL of DMF was added to a slurry of 1.36 g (56.8 mmol) of NaH and 1.0 g of CsCl in 500 mL of DMF by syringe pump over a period of 3 days. After addition was complete, the reaction mixture was stirred for 4 h and 400 mL of dichloromethane was added. The solution was washed and dried as in the preceding preparation. The solvent was removed to leave a sticky oil. Trituration with ether resulted in a solid material, recrystallization of which from hot heptane gave 3.0 g (24%) of pure product as white blocks, mp 102–104 °C. 1H NMR (C_6D_6): δ 1.88 (q, 4), 3.78 (t, 4), 3.80 (t, 4), 3.89 (s, 4), 6.45–6.54 (m, 6), 6.64 (d, 3), 7.10–7.19 (m, 3). FAB-MS (3-nitrobenzyl alcohol): m/e 437 ($M+1$). Anal. Calcd. for $C_{26}H_{28}O_6$: C, 71.54; H, 6.47. Found: C, 71.41; H, 6.42.

(d) **Protected Macrocyclic Polyether Trithiol (6)**. To a solution of 2.0 g (4.6 mmol) of 4 in 200 mL of THF at 0 °C was added dropwise 6.0 mL (17 mmol) of 2.5 M BuLi in hexane. The reaction mixture was raised to 55 °C and maintained at this temperature for 1 h as a deep red color developed. The 1H NMR spectrum of an aliquot of the reaction mixture quenched with D_2O showed that trilitiation was complete at this point. The mixture was maintained at –78 °C while a solution of 3.7 g (15 mmol) of dibenzyl disulfide in 50 mL of THF was added over 1 h. The cold solution was allowed to warm to ambient temperature overnight. (If TLC indicated incomplete consumption of the disulfide, the reaction mixture was maintained at 55 °C for 2–3 h.) The solvent was removed in vacuo, and the residue was dissolved in 400 mL of dichloromethane. The solution was washed with 5% NaOH and with saturated aqueous NaCl and was dried ($MgSO_4$). Solvent removal in vacuo gave a viscous oil, trituration of which with ether afforded 1.8 g (49%) of product as a pale yellow solid, mp 150–152 °C. 1H NMR ($CDCl_3$): δ 2.25 (q, 4), 2.95 (s, 2), 3.69 (s, 4), 4.13 (t, 4), 4.25–4.36 (s/m, 8), 6.23 (d, 2), 6.40

(d, 2), 6.55 (d, 4), 6.83–7.14 (m, 16). FAB-MS (3-nitrobenzyl alcohol): m/e 803 ($M+1$).

(e) **Macrocyclic Polyether Trithiol (7, c-LSH)₃**. To a solution of 1.0 g (1.2 mmol) of 5 in anhydrous liquid ammonia was added small pieces of sodium metal until a blue color persisted. The solution was stirred for 1 h, and the blue color was discharged by careful addition of the minimum amount of NH_4Cl . The ammonia was allowed to evaporate by dinitrogen flow. The white solid residue was dissolved in 40 mL of 2% aqueous NaOH solution at 0 °C. The solution was washed with 40 mL of dichloromethane, cooled to –10 °C, and adjusted to pH 6.0 by addition of concentrated HCl. It was extracted twice with dichloromethane; the combined extracts were dried ($MgSO_4$) and solvent was removed in vacuo, giving a viscous oil or a semisolid. Trituration with ether gave 0.45 g (65%) of pure product as a very pale yellow solid, mp 216–219 °C. The proton labeling scheme is



1H NMR ($CDCl_3$): δ 2.31 (q, 4, γ), 3.83 (s, 1, SH), 3.84 (s, 2, SH), 4.25 (t, 4, β/ϵ), 4.31 (t, 4, ϵ/β), 4.40 (s, 4, α), 6.55–6.62 (6, m, m', m''); 6.97, 7.00 (2t, 4, p, p'). FAB-MS (3-nitrobenzyl alcohol): m/e 533 ($M+1$). Anal. Calcd. for $C_{26}H_{28}O_6S_3$: C, 58.62; H, 5.30; S, 18.06. Found: C, 58.13; H, 5.26; S, 17.31. $Na_3(c-LS_3)$ was generated in solution by the reaction of 7 with 3 equiv of NaSEt in Me_2SO . The chemical shifts of the aromatic protons were required as references for the isotropic shifts of clusters in Me_2SO : δ 6.34 (p, p'), 6.40 (m, m', m'').

Clusters. Isolated cluster compounds were not subjected to elemental analysis owing to the small scale of the preparations. However, their identity and full or substantial purity were established from their 1H NMR spectra. Other clusters were generated in solution and identified from their 1H NMR spectra. These spectra are discussed, and several examples are presented, in the text.

(a) **$(Bu_4N)_2[Fe_4S_4(c-LS_3)(SEt)]$ (8)**. To a solution of 340 mg (0.31 mmol) of $(Bu_4N)_2[Fe_4S_4(SEt)_4]^{14}$ in 50 mL of acetonitrile was added 167 mg (0.31 mmol) of trithiol 7 in 5 mL of chloroform. The reaction was stirred for 1 h and then for another 2 h under dynamic vacuum. Solvent removal in vacuo afforded a quantitative yield of the product as a black solid. 1H NMR (CD_3CN): δ 2.49 (3, SCH_2CH_3); 2.89, 4.35, 4.68, 4.77, 5.18, 6.74 (16, CH_2); 5.52 (1, p), 5.63 (2, p), 7.42 (2, m'), 7.45 (2, m''), 7.71 (2, m), 12.9 (SCH_2). Absorption spectrum (DMF): $\lambda_{max}(\epsilon_M) = 325$ (sh, 14 500), 382 (sh, 12 000), 433 (sh, 10 800) nm.

(b) **$(Bu_4N)_2[Fe_4S_4(c-LS_3)Cl]$ (9)**. To a solution of 166 mg (0.116 mmol) of 8 in 20 mL of acetonitrile was added 12.3 mg (0.102 mmol) of pivaloyl chloride. The reaction mixture was stirred for 45 min and the volume reduced to 10 mL in vacuo. Ether (50 mL) was layered on the solution, and the mixture was allowed to stand overnight. The liquid was decanted to leave an oily solid, which was covered with ether. After this was allowed to stand overnight, the ether was removed to give 120 mg (84%) of product as a microcrystalline black solid. 1H NMR (CD_3CN): δ 2.92, 4.29, 4.62, 4.74, 5.13, 6.34 (16, CH_2); 5.51 (1, p), 5.58 (2, p), 7.37 (2, m'), 7.53 (2, m''), 7.84 (2, m). Absorption spectrum (DMF): $\lambda_{max}(\epsilon_M) = 336$ (sh, 16 600), 380 (sh, 14 300), 437 (11 700).

(c) **$(Bu_4N)[Fe_4S_4(c-LS_3)(t-BuNC)]$ (13)**. To a solution of 10.0 mg (7.10 μ mol) of 9 in 0.5 mL of acetonitrile was added 100 μ L (85 mmol) of a 0.85 M solution of *t*-BuNC in acetonitrile. The reaction mixture was stirred for 30 min, and volatiles were removed to afford the product as a black solid. 1H NMR (Me_2SO): δ 2.07, 4.29, 4.58, 7.35, 9.07, 10.8 (CH_2), –1.01 (p), –1.88 (p), 13.37 (m''), 14.46 (m'), 15.55 (m).

(d) **Clusters Generated in Solution.** Unless noted otherwise, the following clusters were generated in solution by substitution reactions in 10–20 mM solutions of 9 with use of a slight excess (ca. 1.1 equiv) of ligand: $[Fe_4S_4(c-LS_3)(S-p-tol)]^{2-}$ (10, Na(*S-p*-tol)), in 4:1 Me_2SO : $MeCN$ (v/v); $[Fe_4S_4(c-LS_3)(CN)]^{2-}$ (11, (Et₃N)CN); $[Fe_4S_4(c-LS_3)(tacn)]^{-}$ (12, 1,4,7-triazacyclononane); $[(Fe_4S_4(c-LS_3))_2Si]^{4-}$ (14, 0.5 equiv of Li_2S).

(13) Wilson, W. C.; Adams, R. J. *Am. Chem. Soc.* 1923, 23, 528.

(14) Averill, B. A.; Herskovitz, T.; Holm, R. H.; Ibers, J. A. *J. Am. Chem. Soc.* 1973, 95, 3523.

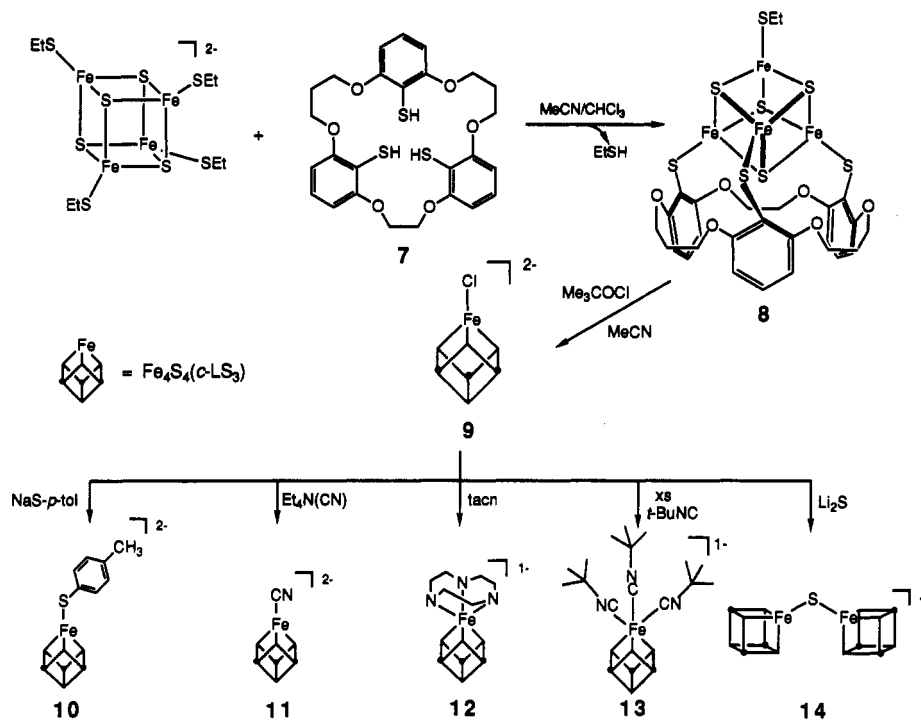


Figure 2. Schematic representations of the structures of subsite-derivatized clusters 8–14 and the reactions by which they are formed.

X-ray Structural Determinations. Crystals of compounds 5 and 6-Et₂O were grown by slow cooling of hot heptane and dichloromethane/ether solutions, respectively. Data were collected on a Nicolet P3F automated four-circle diffractometer using graphite-monochromatized Mo K α radiation. These crystals were of only fair diffraction quality; the data collected were sufficient to determine the molecular structures but not precise bond angles and distances. ω scans were used for data collection for 5 and $\theta/2\theta$ scans for 6-Et₂O. The final orientation matrix and cell parameters were obtained from 25 machine-centered reflections ($20^\circ \leq 2\theta \leq 25^\circ$). Check reflections monitored after every 123 reflections indicated no significant decay over the course of the data collections. Unit cells were checked with the program TRACER, and XTape from the SHELXTL program package was employed for data reduction. No absorption corrections were applied because of the small values of the coefficients μ . For 5, the systematic absences $h0l$ ($l = 2n + 1$) and $0k0$ ($k = 2n + 1$) uniquely define the space group as $P2_1/c$ (No. 14). For 6-Et₂O, the systematic absences $h0l$ ($h + l = 2n + 1$) and $0k0$ ($k = 2n + 1$) uniquely define the space group $P2_1/n$ (No. 14, equivalent positions $\pm(x, y, z; 1/2 - x, 1/2 + y, 1/2 - z)$).

Direct methods (MULTAN) were used to solve the structures. The resorcinol fragments C₆O₂ were included as random groups to aid in the solution of 5; carbon and oxygen atoms from this structure were similarly used as random groups in the solution of 6-Et₂O. The map with the highest figure of merit contained all the non-hydrogen atoms for 5 and most of these atoms for 6-Et₂O. Atom coordinates found from direct methods served as starting points for Fourier refinement using the program CRYSTALS. Atom scattering factors were taken from a standard source.¹⁵ The remaining non-hydrogen atoms of 6-Et₂O were found by Fourier maps. Refinements were carried out in a cascade fashion with large-block approximations to the least-squares matrix. In the later stages of refinement, hydrogen atoms were included at 0.95 Å with isotropic temperature factors 1.2 \times those of the bonded carbon atoms. No hydrogens were placed on the ether solvate. Difference maps of both structures at isotropic convergence were relatively flat with the largest peaks being ca. 0.1 e/Å³. Crystal data and final R values for isotropic refinement are given in Table I. Because precise interatomic distances and angles were not determined, positional parameters are not tabulated but are deposited as supplementary material.¹⁶

Other Physical Measurements. Spectrophotometric, ¹H NMR (500 MHz), and electrochemical measurements were performed under anaerobic conditions by using the equipment and procedures described previously.¹ A glassy-carbon working electrode, 0.1 M (Bu₄N)(ClO₄) supporting electrolyte, a SCE reference electrode, and a scan rate of 50

Table I. Crystallographic Data^a for Cyclic Molecules 5 and 6-Et₂O

	5	6-Et ₂ O
formula	C ₂₆ H ₂₈ O ₆	C ₅₁ H ₅₆ O ₇ S ₃
fw	436.51	877.19
<i>a</i> , Å	10.318 (5)	14.315 (9)
<i>b</i> , Å	17.333 (5)	12.823 (8)
<i>c</i> , Å	13.653 (5)	25.56 (1)
β , deg	111.31 (3)	90.94 (5)
space group	$P2_1/c$	$P2_1/n$
<i>V</i> , Å ³	2274 (2)	4692 (5)
<i>Z</i>	4	4
$\rho_{\text{calcd}}(\rho_{\text{obsd}})$, g/cm ³	1.28 (1.27)	1.24 (1.24)
μ , mm ⁻¹	0.08	0.20
$R(R_w)$, %	8.5 (9.5) ^b	8.1 (8.9) ^b

^aMo K α radiation, $T = 297$ K. ^bWeighting scheme for least-squares refinement: Carruthers, J. R.; Watkin, D. J. *Acta Crystallogr.* 1979, A35, 698.

mV/s were employed in the voltammetric measurements. Under the experimental conditions employed, $E_{1/2}(\text{Fc}^+/\text{Fc}) = +0.45$ V in Me₂SO.

Results and Discussion

Ligand Design. The design aspects of ligand 1 that cause it to form the desired clusters 2 with a 3:1 iron subsite differentiation have been described elsewhere.^{1,2} The 6-Me substituents sterically orient the three coordinating arms such that the majority conformation in solution has the three thiol groups pointing inward, over the central ring. Thus, 1 is a tripodal ligand conformationally predisposed, and also dimensionally correct, for cluster capture. A different approach to a trithiol ligand appropriate for cubane cluster binding utilizes a cyclic structure on which are positioned thiol groups. Molecule 7, depicted in Figure 1, was selected as the synthetic target. It is a crown ether containing three 1-mercapto-2,6-phenylene units. Note that the molecule contains a 3–3–2 pattern of connected methylene groups. A space-filling model of the corresponding 2–2–2 molecule indicated that it is too small to bind three iron subsites of the Fe₄S₄ core without considerable strain and, when bound, places some CH₂CH₂ groups in an eclipsed configuration. By similar means, the 3–3–3 variant was concluded not to fit as snugly around the Fe₄S₄ core as the 3–3–2 ligand, and to be sufficiently flexible to present the possibility of binding to two cores rather than closing on a single core. Use of 1-mercapto-3,5-phenylene units would lead to a molecule of unacceptable conformational flexibility and, therewith, to a high

(15) Cromer, D. T.; Waber, J. T. *International Tables for X-Ray Crystallography*; Kynoch Press: Birmingham, England, 1974.

(16) See the paragraph at the end of this article concerning supplementary material available.

Table II. ^1H NMR Isotopic Shifts and Redox Potentials of $[\text{Fe}_4\text{S}_4(\text{c-LS}_3)\text{L}]^{2-}$ Clusters in Me_2SO at 297 K

L'	$(\Delta\text{H}/\text{H}_0)_{\text{iso}},^a$ ppm					L'	$E_{1/2}(\Delta E_p, \text{V}),^b$ V
	$m\text{-H}$	$m'\text{-H}$	$m''\text{-H}$	$p\text{-H}$	$p'\text{-H}$		
EtS^-	-1.26	-0.88	-0.94	+0.79	+0.93	-10.6 (CH_2), -1.16 (Me)	-1.30 (0.28) ^d
Cl^-	-1.40	-0.83	-1.01	+0.87	+0.96		-1.03 (0.19)
CN^-	-1.37	-0.74	-0.99	+0.79	+0.79		-1.03 (0.21)
$p\text{-tolS}^-^c$	-1.36	-0.97	-1.02	+0.72	+0.82	-1.52 ($m\text{-H}$), +1.83 (Me)	-1.15 (0.18)
tacn	-1.48	-1.11	-1.29	+1.17	+1.20	-6.73, -11.0	-1.26 (0.16)
$(t\text{-BuNC})_3$	-9.21 ^e	-8.09 ^e	-7.03	+8.28	+7.44	+1.10, +1.29	-1.15 (0.18)
S^{2-}	-1.41	-0.85	-1.03	+0.86	+0.96		-1.15 (0.14)
HS^-							-1.28 (0.20)
							-1.23 (0.14)

^a $(\Delta\text{H}/\text{H}_0)_{\text{iso}} = (\Delta\text{H}/\text{H}_0)_{\text{dia}} - (\Delta\text{H}/\text{H}_0)_{\text{obs}}$. ^bVs SCE. ^c4:1 MeCN/Me₂SO (v/v). ^dDMF. ^e $m\text{-H}$ or $m'\text{-H}$.

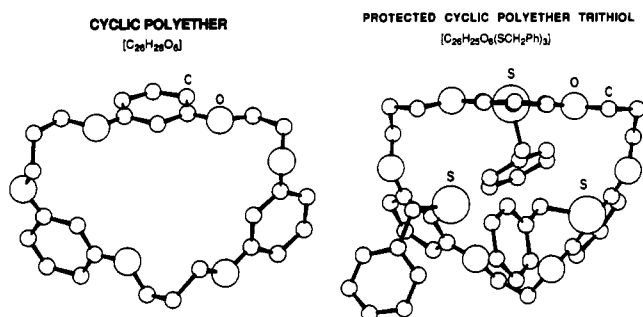
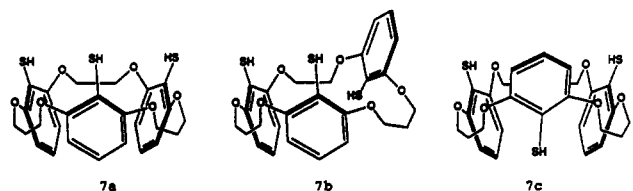


Figure 3. Structures of the cyclic polyether **5** and the protected cyclic polyether trithiol **6** as its ethyl ether monosolvate, obtained from isotropic refinements. Atoms are drawn as spheres of arbitrary radius.

probability of polymer formation.

The 3-3-2 molecule has three main conformational possibilities. In **7a**, the three thiol groups are on the same side of the mean plane of the six oxygen atoms and the molecule is in a conformation (aaa)¹⁷ of C_3 symmetry prepared for cluster binding. The remaining conformation (aab), with two thiol groups above and one below the O_6 approximate plane, has two isomers, **7b,c**, owing



to the 2:1 equivalence of the phenyl rings. The conversion aab \rightarrow aaa is required if the molecule is to bind to a single cluster.

Ligand Synthesis. The synthetic scheme is set out in Figure 1. The critical step is the high-dilution cyclization¹⁹ of resorcinol derivatives **3** and **4** to form the tris(1,3-phenylene) crown ether **5**, which has been obtained in 24% yield. The X-ray structure of this compound is shown in Figure 3. Its cyclic nature is immediately apparent; the molecule contains a 23-membered ring. Because the C(2)-H groups of the three 1,3-phenylene rings, which are tilted toward one another, lie above the O_6 mean plane, the molecule has the aaa conformation. A few macrocycles containing fragments derived from resorcinol have been prepared and structurally characterized,¹⁹⁻²¹ but none contain three such fragments as does **5**.

Crown ether **5** was lithiated and converted to the protected trithiol **6** in 49% yield by reaction with dibenzyl disulfide. The

identity of **6** was demonstrated by an X-ray structure determination of the ethyl ether monosolvate, shown in Figure 3. In this case the ring conformation is aab, which is undoubtedly adopted to avoid interactions of three benzyl groups on the same side of the molecule. The two sulfur atoms on the same side of the central ring are separated by 5.2 Å. Thus the ring structure represented by **5** can adopt either aab conformation, but from space-filling models, it is unlikely that **6** can interconvert between the two because the benzyl groups are too large. Metric parameters and ring torsional angles of **5** and **6** are given elsewhere.¹⁶

Deprotection of **6** by standard means affords the desired trithiol **7** in 65% yield, or in 8% yield from the readily prepared resorcinol derivatives **3** and **4**. The compound was fully identified spectroscopically. The ^1H NMR spectrum at ambient temperature in three solvents (CDCl_3 , CH_2Cl_2 , $\text{CD}_3\text{CN}/\text{Me}_2\text{SO}$) is consistent with C_3 symmetry and has been fully assigned from signal intensities and COSY experiments. The ^1H NMR spectrum in CD_2Cl_2 at 210 K is unchanged from that at 297 K except for slight line broadening. There is no direct evidence for unsymmetrical isomer **7b** or for the presence of both C_3 isomers, **7a** and **7c**, at slow exchange. We are unable to distinguish between **7a** or **7c** alone or as a rapidly interconverting isomer mixture, although the latter seems unlikely from the low-temperature spectrum. Diffraction-quality crystals of **7** have not been obtained.

Cluster Capture Reaction. Equimolar reaction of $[\text{Fe}_4\text{S}_4(\text{SEt})_4]^{2-}$ and trithiol **7** in chloroform/acetonitrile (10:1 v/v) proceeds by ligand substitution to afford $[\text{Fe}_4\text{S}_4(\text{c-LS}_3)(\text{SEt})]^{2-}$ (**8**), which was isolated in essentially quantitative yield as a black solid. The success of this reaction suggests that the trithiol exists entirely in form **7a** or that a labile mixture of conformers is readily shifted toward this form upon cluster binding. Although we have not been able to isolate crystals suitable for X-ray structural determination, proof of structure **8** as depicted in Figure 2 follows from the ^1H NMR spectrum of the cluster.

The NMR spectra of cluster **8**, shown in Figure 4 at three temperatures in acetonitrile solution, reveal the standard NMR properties of $[\text{Fe}_4\text{S}_4]^{2+}$ clusters; viz., decreasing isotropic shifts with decreasing temperature, and oppositely signed meta H and para H isotropic shifts.²² The assignments given for this and subsequent clusters follow from those of $[\text{Fe}_4\text{S}_4(\text{SR})_4]^{2-}$ ($\text{R} = \text{Et}, \text{Ph}$), relative signal intensities, and COSY and variable-temperature experiments. Spectral resolution usually depends on temperature. Thus at 298 K three meta H and two para H signals are observable; resolution of the former in terms of three equally intense signals occurs at 253 K. Further, there are five ligand CH resonances evident in the 4-7 ppm interval and an additional signal near 2.5 ppm (not shown). We conclude that trithiol **7** functions as a tridentate ligand, affording the site-differentiated cluster **8**, which serves as a starting point for the investigation of subsite-specific ligand substitution reactions. The NMR results

(17) This nomenclature (a, "above"; b, "below") is that used previously to describe the conformations of hexasubstituted benzenes.^{1,2,18}

(18) MacNicol, D. D.; Mallinson, P. R.; Robertson, C. D. *J. Chem. Soc., Chem. Commun.* **1985**, 1649.

(19) Weber, E. *Prog. Macrocyclic Chem.* **1987**, *3*, 337.

(20) Weber, E.; Josel, H.-P.; Puff, H.; Franken, S. *J. Org. Chem.* **1985**, *50*, 3125.

(21) Chacko, K. K.; Ruban, G. A.; Aoki, K.; Weber, E. *Acta Crystallogr.* **1988**, *C44*, 352.

(22) Clusters containing the $[\text{Fe}_4\text{S}_4]^{2+}$ core normally have an $S = 0$ ground state, excited paramagnetic states that are thermally populated, and isotropic shifts of terminal thiolate ligands that are mainly or entirely contact in origin.²³

(23) (a) Holm, R. H.; Phillips, W. D.; Averill, B. A.; Mayerle, J. J.; Herskovitz, T. *J. Am. Chem. Soc.* **1974**, *96*, 2109. (b) Reynolds, J. G.; Laskowski, E. J.; Holm, R. H. *J. Am. Chem. Soc.* **1978**, *100*, 5315.

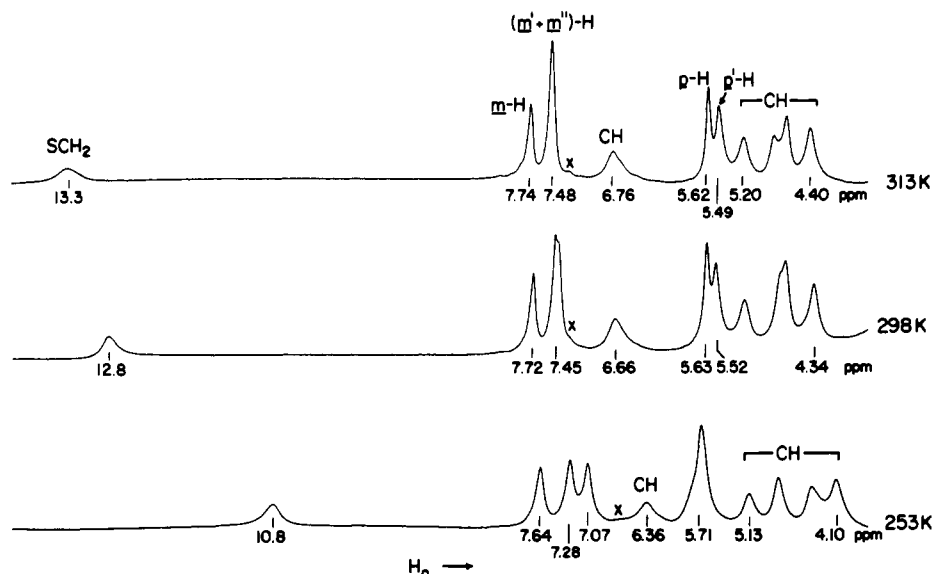


Figure 4. ^1H NMR spectra of isolated cluster **8** in CD_3CN solution at 253–313 K. In this and subsequent figures, signal assignments are indicated: CH = ligand methylene proton(s), and x = impurity.

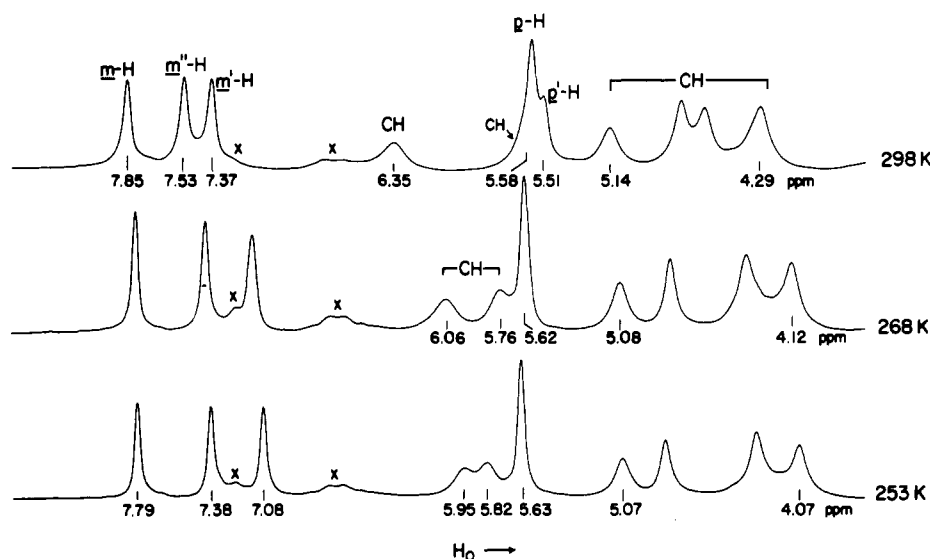


Figure 5. ^1H NMR spectra of isolated cluster **9** in CD_3CN solution at 253–298 K. The impurity was persistent in different preparations and difficult to remove, and appears in the spectra of Figure 6.

are consistent with cluster mirror symmetry, in which protons of individual methylene groups of the ligand are rendered inequivalent by cluster binding. Only four different types of methylene protons are observed for trithiol **7** and its trisodium salt.

Subsite-Specific Reactivity. Cluster **8** contains subsites differentiated in the desired 3:1 ratio and, as will be shown, undergoes an electrophilic substitution reaction at the unique subsite. This and related reactions are most effectively monitored by ^1H NMR spectroscopy, taking advantage of the sensitivity of isotropic shifts to the variant ligand L' of $[\text{Fe}_4\text{S}_4(\text{c-LS}_3)L']^{2-}$ in the same manner as used to detect the formation of the clusters **2**.^{1–7} Redox potentials also depend on the identity of L' and provide another means of detecting ligand substitution. Isotropic shifts and potentials for the core redox reaction $[\text{Fe}_4\text{S}_4]^{2+/+}$ for cluster **8** and some six other species in Me_2SO solutions are set out in Table II for comparison purposes. In general, isotropic shifts show a small solvent dependence in acetonitrile, DMF, and Me_2SO solutions. The new clusters and the reactions that afford them are schematically depicted in Figure 2.

(a) NMR Results. Reaction of **8** with pivaloyl chloride in acetonitrile solution afford the monochloride cluster **9**, which was isolated. The ^1H NMR spectra of this cluster, shown at three temperatures in Figure 5, provide better spectral resolution than in the case of **8** and demonstrate the sensitivity of both ring and

methylene resonances to ligand variation at the unique subsite. Three meta H resonances are fully resolved at all temperatures and two para H signals are observable at 298 K, consistent with mirror symmetry. Further, at the two lower temperature, signals of at least six of the eight inequivalent methylene protons are resolved.

Cluster **9** readily undergoes substitution reactions upon treatment with ca. 1 equiv of ligand L' at ambient temperature. Addition of *p*-toluenethiolate leads to cluster **10**, whose formation is demonstrated by the appearance of a fourth meta H signal (7.97 ppm) and a methyl resonance with negative and positive isotropic shifts, respectively. Similarly, reaction with cyanide yields **11** and tacn produces **12**; spectra at 297 K are given in Figure 6. That of **11** differs slightly from the spectrum of **9** and contains five to six methylene resonances at 4–6.5 ppm. The formation of **12** is made obvious by the inequivalence of the tacn methylene protons, which give rise to the broad signals at 9.18 and 13.1 ppm.

Reaction of **8** with excess *t*-BuNC affords a cluster with the well-resolved spectrum in Figure 7. Note that the meta H and para H isotropic shifts are ca. 7–10 times larger than those of an $S = 0$ cluster such as **8**. A similar behavior has been previously encountered in the reaction of cluster **2** ($L' = \text{Cl}^-$) with excess isonitriles, including *t*-BuNC.⁷ As in those cases, signal integration shows the binding of three isonitrile molecules, which are in slow

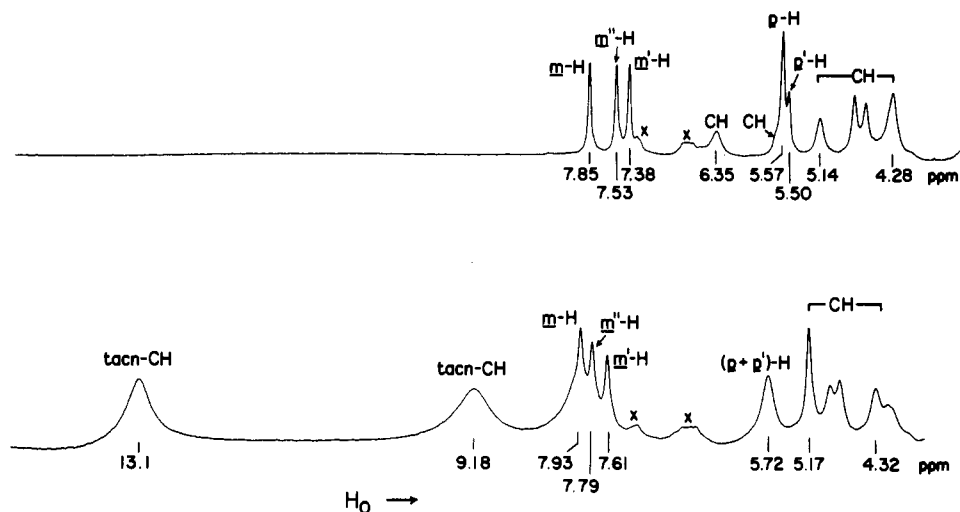


Figure 6. ^1H NMR spectra of clusters **11** (top) and **12** (bottom) generated in situ at 297 K. The signal underlying the meta H resonances of **12** (CH or NH?) has not been identified.

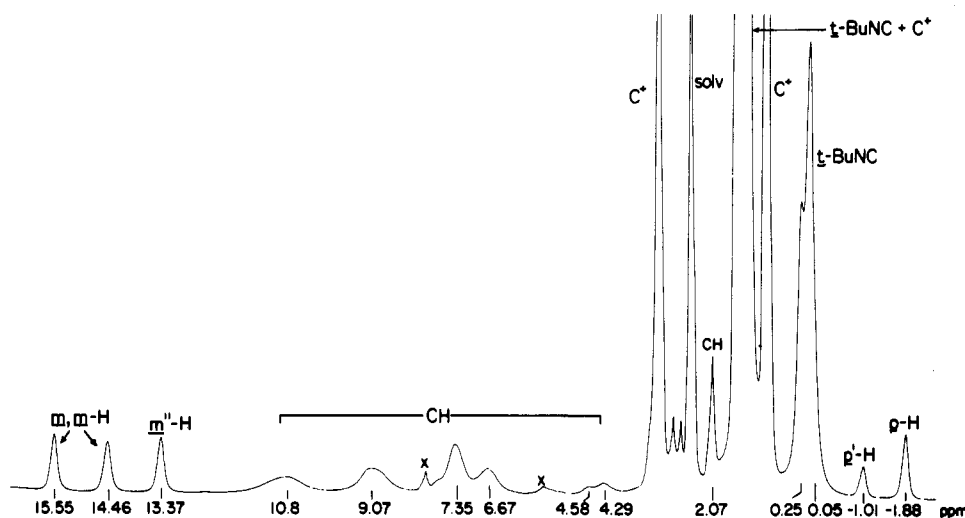


Figure 7. ^1H NMR spectrum of isolated cluster **13** at 297 K ($\text{C}^+ = \text{Bu}_4\text{N}^+$), illustrating the large chemical shifts arising from the presence of the Fe_3S_4 ($S = 2$) cluster fragment.⁷

exchange with the unbound fraction. In the present case, the bound isonitriles are inequivalent (0.05, 0.23 ppm), a finding that together with the pattern of meta H and para H resonances provides a decisive indicator of the mirror symmetry of cluster **13**. From the large isotropic shifts, we conclude that **13** has the same electronic structure as **2** ($L' = (\text{RNC})_3$); viz., the unique subsite is low-spin Fe^{II} , and the $[\text{Fe}_3\text{S}_4]^0$ core remainder is a spin-isolated fragment with $S = 2$.

Treatment of **8** with $1/2$ equiv of Li_2S affords a species whose ^1H NMR spectrum (not shown) resembles that of the precursor cluster but with small changes in isotropic shifts. Three meta H and two para H signals are fully resolved, and at least six CH signals are observed at 4–7 ppm. Together with the voltammetric data (vide infra), these results identify the reaction product as the sulfide-bridged cluster **14**.

(b) Voltammetry. As seen from the cyclic voltammogram in Figure 8, both core redox couples $[\text{Fe}_4\text{S}_4]^{2+/+}$ and $[\text{Fe}_4\text{S}_4]^{3+/2+}$ are stabilized by the cyclic ligand in dichloromethane solution. In other solvents, the latter couple is irreversible or not well defined. The former couple is observed in all solvents; potentials, mainly in Me_2SO solutions, are entered in Table II. At parity of ligand L' and solvent, potentials of $[\text{Fe}_4\text{S}_4(\text{c-LS}_3)L']$ couples are, with one exception, ca. 0.10–0.15 V more negative than those of $[\text{Fe}_4\text{S}_4(\text{LS}_3)L']$ couples. These couples are chemically reversible ($i_p/i_a \approx 1$), but the very large differences in peak potentials imply slow electron transfer at the electrode.

In the case of the sulfide reaction product, the observation of two redox processes separated by 130 mV is tentative evidence

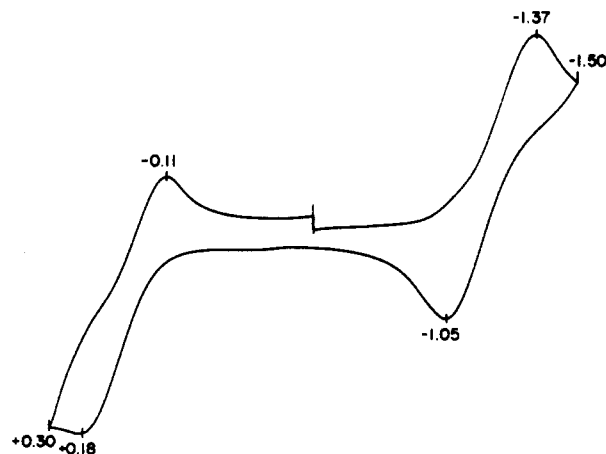


Figure 8. Cyclic voltammogram (50 mV) of cluster **8** in dichloromethane solution, illustrating the redox steps $[\text{Fe}_4\text{S}_4]^{2+/+}$ ($E_{1/2} = -1.21$ V) and $[\text{Fe}_4\text{S}_4]^{3+/2+}$ ($E_{1/2} = +0.04$ V). Peak potentials vs SCE are indicated.

for the existence of the double cubane **14**. Neither process is due to another conceivable product, $[\text{Fe}_4\text{S}_4(\text{c-LS}_3)(\text{SH})]^{2-}$, whose redox reaction occurs at a different potential (Table II). The double cubane $\{[\text{Fe}_4\text{S}_4(\text{LS}_3)]_2\text{S}\}^{4-}$ has been generated in Me_2SO solution and exhibits two redox steps separated by 220 mV.⁵ The viability of a sulfide-bridged double cubane has been demonstrated by the preparation and structure determination of $\{[\text{Fe}_4\text{S}_4\text{Cl}_3]_2\text{S}\}^{4-}$.²⁴ The

intercluster Fe-S-Fe angle is 102° , and the difference in potentials of the two redox processes is 300 mV (acetonitrile). By a redox potential criterion, individual clusters in the three double cubanes are electronically coupled in the order of increasing potential separations. With **14** and $\{[\text{Fe}_4\text{S}_4(\text{c-LS}_3)]_2\text{S}\}^{4+}$, ligand bulk presumably causes the intercluster angle to exceed that in $\{[\text{Fe}_4\text{S}_4\text{Cl}_3]_2\text{S}\}^{4+}$. We are unable to explain why the first reduction potential of **14** (-1.15 V in DMF) is more positive than that of $\{[\text{Fe}_4\text{S}_4(\text{LS}_3)]_2\text{S}\}^{4+}$ (-1.28 V in Me_2SO^2). Because formulation of **14** is based only on redox behavior, it must be considered less certain than that of the other clusters in Figure 2.

Summary. The following are the principal results and conclusions of this investigation.

(1) The new macrocyclic polyether trithiol **7** can be prepared in 49% yield from crown ether **5**, whose cyclic structure has been proven by X-ray analysis, and in 8% yield from precursors **3** and **4**. Because of multiple preparations, these are near-optimized yields.

(2) Trithiol **7** quantitatively captures the cluster $[\text{Fe}_4\text{S}_4(\text{SEt})_4]^{2-}$ in solution to afford the subsite-differentiated cluster $[\text{Fe}_4\text{S}_4(\text{c-LS}_3(\text{SEt}))]^{2-}$ (**8**), which has been isolated in quantitative yield and may be converted in high yield to chloride cluster **9**.

(3) Cluster **9** sustains subsite-specific substitution reactions with a slight stoichiometric excess of ligand to afford clusters **10-12** and **14**. A ca. 10-fold excess of ligand is required to form isonitrile cluster **13** in an equilibrium reaction.

(4) Properties of subsite-differentiated clusters $[\text{Fe}_4\text{S}_4(\text{c-LS}_3)\text{L}']^{2-}$ (**8-14**), while not identical, are sufficiently similar to those of $[\text{Fe}_4\text{S}_4(\text{LS}_3)\text{L}']^{2-}$ (**2**) at constant L' to suggest that neither tridentate ligand imposes a highly specific environment on the Fe_4S_4 core. Consequently, either ligand may be utilized for a given purpose in chemistry of subsite-differentiated clusters, with the properties of resultant new species having different trithiolate ligands being reasonably comparable.

The results in Figure 2 constitute the second set of examples of subsite-specific substitution reactions of $[\text{Fe}_4\text{S}_4]^{2+}$ clusters. The previously described substitution reactions of the clusters **2**^{1,2,5-7} have been considerably expanded and will be reported elsewhere.⁴ Point 4 indicates that either ligand system affords a suitable simulation of coordination in the $\text{Fe}_4\text{S}_4(\text{S-Cys})_3$ cluster unit proven by protein crystallography in aconitase.¹¹ Consequently, the clusters $[\text{Fe}_4\text{S}_4(\text{c-LS}_3)\text{L}']^{2-}$ and $[\text{Fe}_4\text{S}_4(\text{LS}_3)\text{L}']^{2-}$ may find further use in the creation of physiologically relevant ligand binding at the unique subsite and in the stabilization of the cuboidal Fe_3S_4 core. Experiments related to these matters are underway.

Acknowledgment. This research was supported by NIH Grant GM 28856. X-ray diffraction equipment was obtained by NIH Grant 1 S10 RR 02247. We thank J. A. Weigel, Dr. H. E. Nordlander, and Dr. T. D. P. Stack for helpful discussions.

Supplementary Material Available: X-ray crystallographic data for the compounds in Table I, including tables of intensity collections and structure refinement parameters, atom positional and isotropic thermal parameters, and bond distances and angles (8 pages); tables of calculated and observed structure factors (27 pages). Ordering information is given on any current masthead page.

(24) Challen, P. R.; Koo, S.-M.; Dunham, W. R.; Coucouvanis, D. *J. Am. Chem. Soc.* **1990**, *112*, 2455.